We are IntechOpen, the world's leading publisher of Open Access books Built by scientists, for scientists

4,800
Open access books available

122,000
International authors and editors

135M
Downloads

Our authors are among the

154
Countries delivered to

TOP 1%
most cited scientists

12.2%
Contributors from top 500 universities

CLARIVATE ANALYTICS BOOK CITATION INDEX INDEXED

WEB OF SCIENCE™

Selection of our books indexed in the Book Citation Index in Web of Science™ Core Collection (BKCI)

Interested in publishing with us?
Contact book.department@intechopen.com

Numbers displayed above are based on latest data collected.
For more information visit www.intechopen.com

4

Fundamental Experiments of Coal Ignition for Engineering Design of Coal Power Plants

Masayuki Taniguchi
Hitachi Research Laboratory, Hitachi, Ltd.
7-1-1 Omika-cho, Hitachi-shi, Ibaraki-ken,
Japan

1. Introduction

1.1 Background

Pulverized fuel combustion systems are widely used in thermal power plants. Plant performances vary with solid fuel properties, but it is difficult to evaluate the effects of fuel properties using large scale facilities. Fundamental experimental techniques are required to evaluate the effects for actual systems. Small scale experiments are comparatively low-priced and simple, and they require a comparatively short time and small amount of coal. In the present study, we focused on ignition properties. First, we developed a fundamental experimental technique to examine ignition performances of various coals. Then, we examined the common point and the differences of ignition phenomena of the actual systems by fundamental experiments. Finally, some application examples were considered.

Ignition properties are fundamental combustion performance parameters for engineering design of combustion systems. Many fundamental research studies have been carried out regarding coal ignition. Ignition temperature, flammability limit concentration (explosion limit concentration) and burning velocity (flame propagation velocity) are important ignition performance parameters. We examined a technique for getting these fundamental ignition parameters to apply burner design for pulverized fuel combustion systems.

The ignition temperatures of coals have been extensively measured. For example, a thermogravimetric technique [1, 2] and an electrically heated laminar-flow furnace (drop-tube furnace) technique [3] have been used. The ignition temperature is useful to grasp differences in fuel properties and surrounding gas compositions. However, there are some problems for applying the ignition temperature data to actual burner designs. For example, the ignition temperature sometimes decreases when the particle diameter is increased. Such results would lead to the idea that flame stabilization becomes easy when particle diameter is increased. However, decreasing the particle diameter is very important to obtain a stable flame for actual burner systems.

In industries handling powders, the prevention of dust explosions is important for ensuring safety. Measuring the explosion limit concentration is important and some standard experimental devices have been applied to this [4, 5]. Explosion limit concentration has been measured for various coals and experimental conditions. It is technically difficult to raise fuel concentration for a pulverized coal firing boiler, so measurement of the lean explosion

limit concentration is important. Generally, lean explosion limit concentration is low when the particle diameter is fine [4]. This tendency accords with the phenomenon experienced in actual systems. Explosion limit concentrations are basic data for burner designs. At the very least, coal concentration should be larger than the lean explosion limit concentration. However, there are two problems for application.

1. The flames formed by explosion limit experiments are unsteady. It is necessary to clarify common points and differences with the continuously formed burner flame.
2. Influence of heat loss on flame stability is large for pulverized coal flames.

For actual boilers, the coal flames are surrounded by the furnace wall. The furnace wall temperature is several hundred degrees Celsius for a water wall, and it is larger than one thousand degrees Celsius for a caster wall. On the other hand, wall temperatures are usually room temperature for the experimental devices used to measure explosion limit. It is necessary to establish a procedure to correct for the influence of heat loss from the flame to surroundings.

Burning velocity (flame propagation velocity) has been used widely for gas combustion as a basic physical quantity [6, 7]. Burning velocity affects the burner design. Generally, velocity of fuel and air injected from the burner are regulated in response to burning velocity. However, there have been only a few studies about these topics for pulverized coal combustion. Flame propagation velocities of pulverized coals were measured in the microgravity condition [8, 9]. Fujita et al. [8] examined the effect of surrounding oxygen concentration and pressure on flame propagation velocity, while Suda et al. [9] examined flame propagation velocities for oxy-fuel combustion conditions. Chen et al. [10] and Taniguchi et al. [11] developed laser ignition equipment to examine flame propagation velocity of pulverized coals. As well, Taniguchi et al. [12] examined the relationship between flame propagation velocity and lean flammability limit for various coals.

In the present study, we introduce procedures to apply these fundamental experiment results to burner design. A basic model of the flame propagation was examined at first. Then, effects of experimental conditions, such as coal properties, particle diameters, and surrounding gas compositions, were examined. The laser ignition experiments provided an unsteady flame. Ignition phenomena obtained with the laser ignition experiments were compared with those of continuous flames. Some correction procedures were introduced to apply the fundamental data to actual burner designs. Finally, a case study was introduced to obtain stable combustion for some biomass fuels.

1.2 Ignition and flame propagation phenomena for pulverized coal combustion

Recently, reduction of CO_2 emissions is required for coal fired thermal power plants. To achieve this, various approaches have been taken. Ultra supercritical power plants have been developed for improvement of power efficiency [13]. Oxy-fuel combustion technology is being pursued for carbon capture and storage [14]. Further reduction of the environmental load, such as NOx reduction, is also still required [15].

Numerical simulations such as computational fluid dynamics (CFD), are very important to design such new technologies. Figure 1 shows an example of a CFD calculation for a pulverized coal firing boiler [16-18]. The temperature distribution is shown in the figure as well as examples of items targeted for the evaluation. Numerical analyses were first applied to evaluate heat absorption by the furnace wall [19], since then they have been applied to such environmental performance factors as NOx emission [20, 21] and to control furnace wall corrosion [22]. Evaluation of flame stability, such as prediction of blow-off limit, is possible, but, this evaluation is relatively difficult [23, 24].

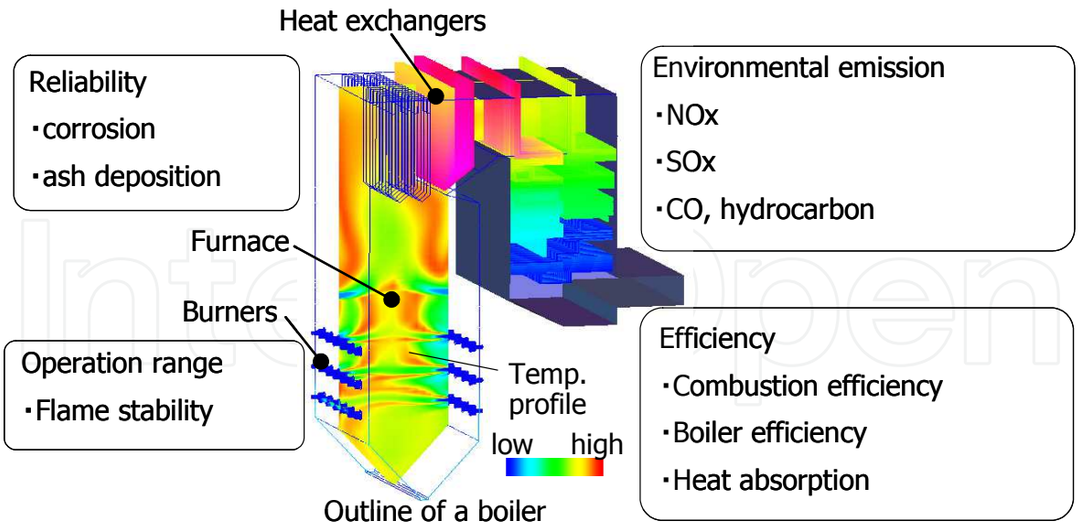

Fig. 1. Schematic of a pulverized coal fired boiler and results that can be calculated by using CFD.

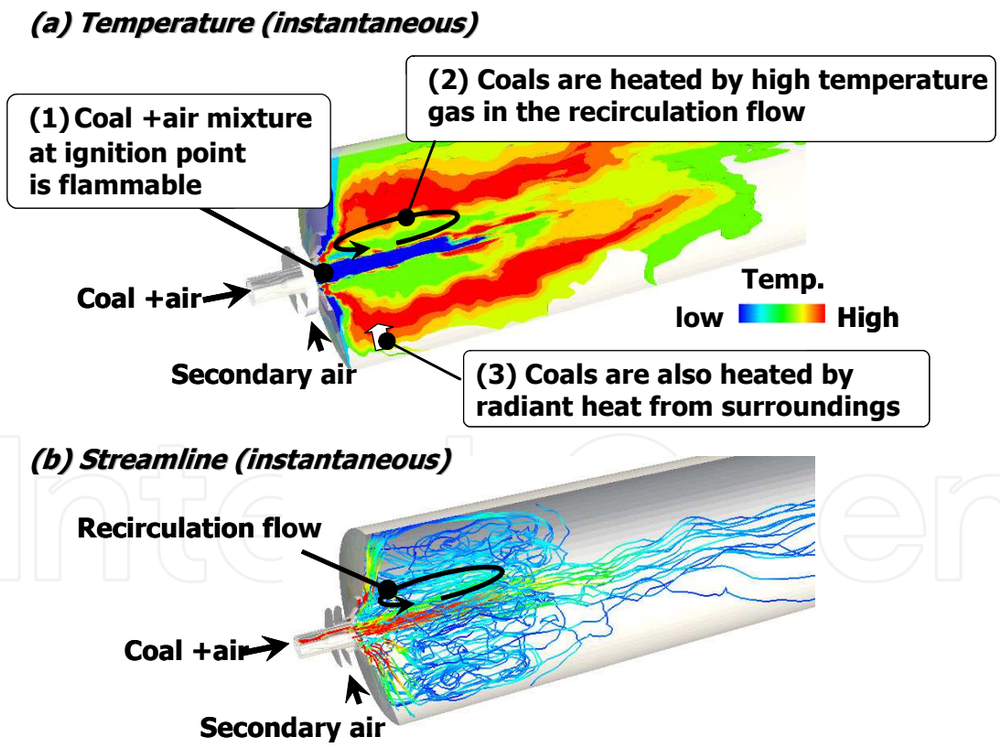

Fig. 2. Examples of detailed calculated results of pulverized coal combustion.

Figure 2 shows the temperature distribution (a) and streamlines (b) in a burner neighborhood. A recirculation flow is formed around the burner exit. Pulverized coals are ignited by the high temperature gas in the recirculation flow. It is necessary to meet following three conditions to form a stable flame.

1. The coal + air mixture at the ignition point is flammable.
2. Coal particles are heated by high temperature gas in the recirculation flow.
3. Coal particles are also heated by radiant heat from the surroundings.

The conditions (1) and (3) were investigated by fundamental experiments. Flame stability can be examined more precisely by combining the fundamental experiments and CFD calculations.

Table 1 lists examples of coals used for power plants and their properties that were examined. Recently, the range of studied fuel properties has been spreading. The establishment of combustion technology that can support a wide range of fuel properties is required.

Fuel type	Higher calolific value	volatile matter	Fixed carbon	ash	C	H	O	N	S
	(MJ/kg, dry)	(wt%, dry)			(wt%, dry ash-free)				
biomass	19.7	76.4	20.4	3.2	49.8	6.3	43.5	0.4	0.01
Lignite	26.5	36.8	35.2	28.0	70.7	4.9	23.1	1.0	0.3
sub-bituminous	26.9	44.5	41.4	14.1	76.3	6.4	15.3	1.3	0.7
sub-bituminous	27.2	42.5	49.0	8.5	69.1	5.4	23.8	1.1	0.6
hv-bituminous	32.4	37.6	55.1	7.3	83.6	5.5	7.7	1.6	1.5
hv-bituminous	29.7	32.5	53.2	14.3	83.4	5.4	8.8	1.9	0.5
mv-bituminous	30.9	21.8	70.8	7.4	87.6	4.7	4.9	2.1	0.8
lv-bituminous	29.3	14.3	68.8	16.9	89.0	4.3	4.6	1.6	0.4
petroleum coke	36.8	11.8	85.9	2.5	86.3	3.9	1.3	2.9	5.7

Table 1. Examples of coal used for power plants and their properties

Object of this chapter is to develop a model to predict lean flammability limit and flame propagation velocity for pulverized solid fuels, and to apply the model to engineering design for burner systems.

2. Laser ignition experiments

2.1 Experimental equipment

Figure 3 shows a schematic of the laser ignition equipment [10-12, 25]. Uniformly sized pulverized coal particles were suspended in a laminar upward flow and rapidly heated by a single-pulsed YAG laser. Velocity of the upward flow was controlled according to the particle diameter. The heated pulverized coal particles were burned in the quartz test section (50mm cross section area). Emissions from the igniting and burning particles were detected with three photomultiplier tubes (PMTs) and the events were concurrently recorded with a high speed camera.

A He-Ne continuous sheet laser (sheet width 3x10 mm; energy flux around $2x10^{-2}$ W/m^2) was irradiated horizontally at the ignition point. The particle concentration was measured from the intensity of particle scattering by the He-Ne laser. Another continuous laser (copper vapor laser: maximum laser power 15W; wavelength 488 and 515 nm) was used to reveal the effect of radiant heat loss on the ignition characteristics. The radiant heat loss was

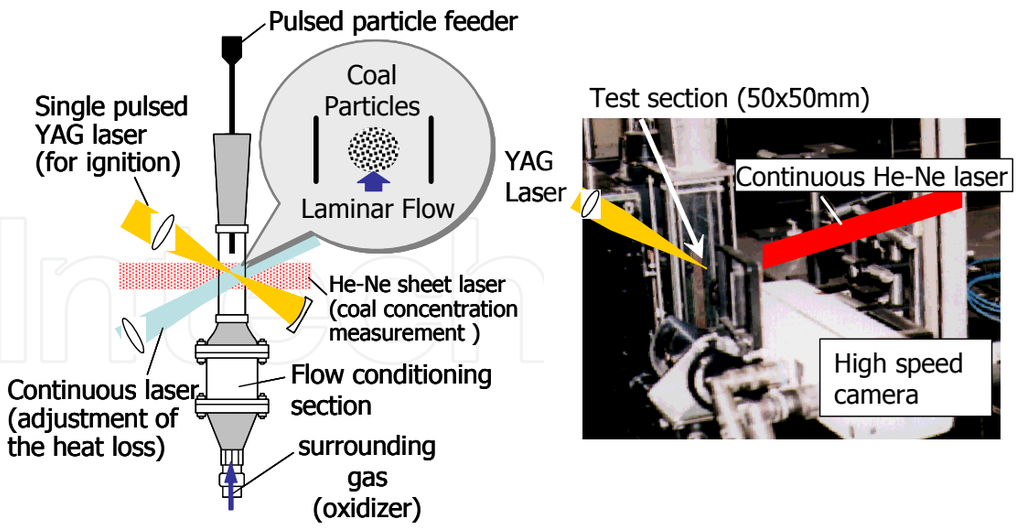

Fig. 3. Schematic drawing of laser ignition experiments

larger for the basic equipment because the quartz wall of the cross-sectional area was kept at room temperature. The effect of radiant heat loss was examined by varying the energy flux of the copper vapor laser. The laser beam was supplied through an optical fiber. The beam diameter was controlled using a collimating lens and concave mirror. Usually, the beam diameter was 15 mm around the ignition point.

The advantage of the laser ignition experiments is the ability to observe ignition phenomena which are similar to actual combustion phenomena, by using a very little amount of coal sample. Both flame propagation velocity and lean flammability limit can be obtained. Observed flame images are shown in Fig.4. Flame propagation velocity was analyzed by increasing the flame radius [11]. Photos of the flame of a hv-bituminous coal (high volatile content) and a lv-bituminous coal (low volatile content) are shown in the figure. The flame of the hv-bituminous coal grew faster than that of the lv-bituminous coal. Flame propagation velocity was large when volatile content was high. Both flames of fine particles and coarse particles are shown for lv-bituminous coal. When particle diameter was fine, flame propagation velocity was large. Lean flammability limit was analyzed by measuring the lower limit of particle concentration at which the flame could grow [11]. When coal concentration was high; almost the same as that for actual systems, the flame moves from the particle directly heated by the pulsed YAG laser to neighboring particles; in this way the flame grew. We defined these phenomena as flame propagation [11, 25]. Only particles directly heated by the pulsed laser burned when the coal concentration was low. Under this condition, we could observe ignition phenomena of a single particle [10, 26].

It is important to have particles stand still as much as possible, in order to obtain reproducible data. Prior to experiments, we observed the stationary state of the particles. Figure 5 shows photos of floating particles near the ignition point when suspended in N_2 flow. Scattering of the He-Ne sheet laser was used for observation. Particles were scattered symmetrically judging from the photos. Particle concentration was evaluated by the intensity of scattering light. Optimum velocity of the upward flow and timing of the laser irradiation were decided, so that variation of particle concentration with time became small just before the YAG laser irradiation.

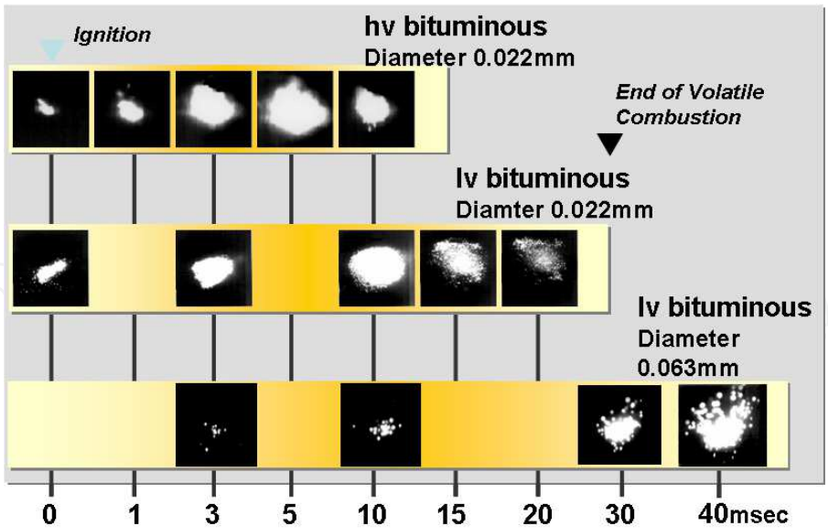

Fig. 4. Examples of flame propagation phenomena obtained from the laser ignition experiments.

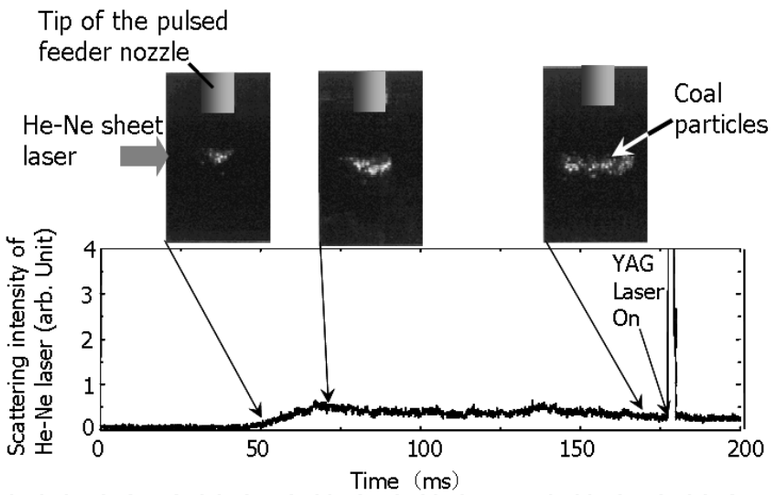

Fig. 5. Observation of floating particles.

2.2 Basic model for ignition and flame propagation

Figure 6 summarizes the basic phenomena of flame propagation. One of two particles burns first, then, the other particle is ignited by the heat of combustion of the one burning particle. When the first particle ignites, volatile matter is pyrolized. A volatile matter flame is formed around the first particle. The flame grows due to volatilization, and the flame heats the next particle which has not ignited yet. Flame propagation is observed if the first burning particle can transfer the flame to the next particle before the volatile matter combustion of the first particle has finished. We defined the distance between particles as d and the time of flame propagation as s. Flame propagation velocity Sb was defined as the value of d divided by s. Relationships between d and s under various experimental conditions were analyzed.

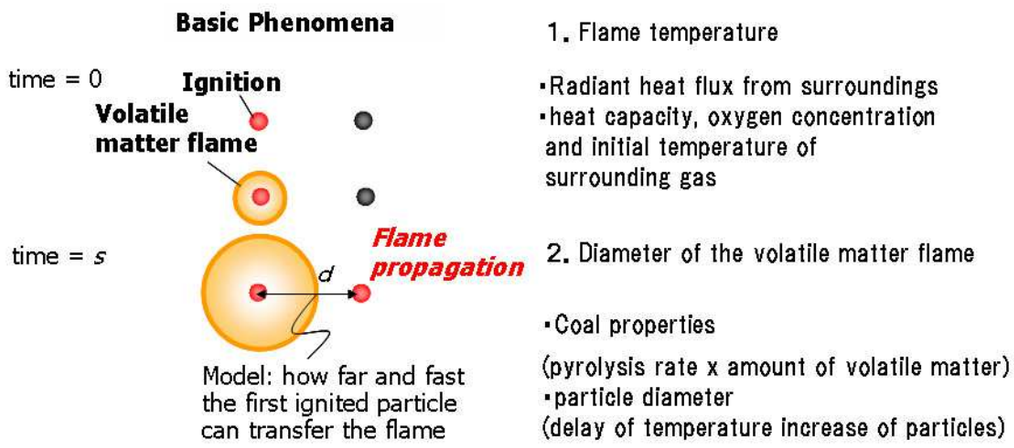

Fig. 6. Basic model for flame propagation.

An example relationship between coal concentration and flame propagation velocity is shown in Fig.7 [12]. Coal concentrations and flame propagation velocities are shown as normalized values. The coal concentration was in inverse proportion to the third power of the distance *d*. When the coal concentration increased, flame propagation velocity increased. But there was an upper limit value (*Sb-max*) to the flame propagation velocity. The flame propagation velocities were almost zero at the lean flammability limit. Absolute values of *L* and *Sb-max* were found to vary with coal properties and burning conditions. An example relationship between *L* and *Sb-max* is shown in Fig. 8. Lean flammability limit; *L* was inversely proportional to maximum flame propagation velocity; *Sb-max* [12].

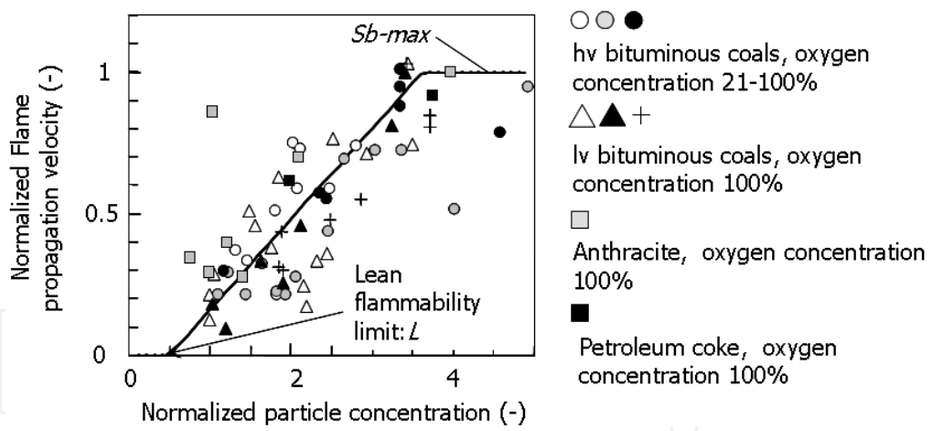

Fig. 7. Relationship between coal concentration and flame propagation velocity [12].

Data on bituminous coals and anthracites of the same particle diameter were obtained under various burning conditions [12], and the effect of particle diameter was examined [11, 25]. Relationships between *L*, *Sb-max* and particle diameter *Dp* are summarized by Eqs. (1)-(3).

$$Sb\text{-}max \propto 1 / L \tag{1}$$

$$L / Sb\text{-}max \propto Dp^2 \tag{2}$$

$$L \propto Dp^{1.5} \tag{3}$$

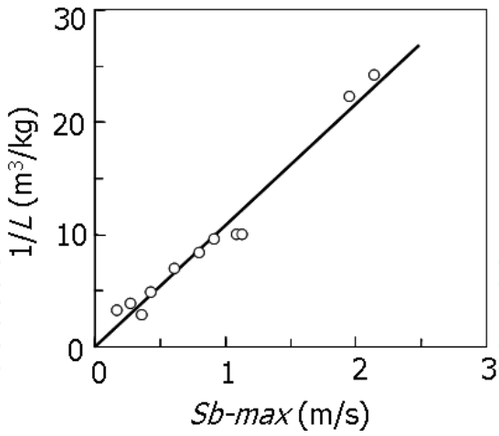

Fig. 8. Relationship between maximum flame propagation velocity *Sb-max* and lean flammability limit *L* [12].

2.3 Effects of experimental conditions on flame propagation performances for laser ignition experiments

Ignition properties of solid fuel vary significantly with fuel properties. One of the most important things is to keep the fuel concentration within the flammable condition, to form a stable flame. Effects of fuel properties on lean flammability limit were examined experimentally at first. Figure 9 shows the lean flammability limit L at the same diameter with different volatile contents of coals. The evaluation method of lean flammability limit has been shown elsewhere [11, 25]. The vertical axis of Fig. 9 is the reciprocal of the lean flammability limit concentration. Lean flammability limits were low for high volatile coals.

The growth rate of the volatile flame is usually large for high volatile coals, because the pyrolysis rate is usually large. The flame propagation time *s* in Fig. 6 was short. The amount of volatile matter was large for high volatile coals, so that the volatile flame which formed around a particle became large. The flame could be transmitted in a short time from one burning particle to another, even though the distance between the particles *d* was large.

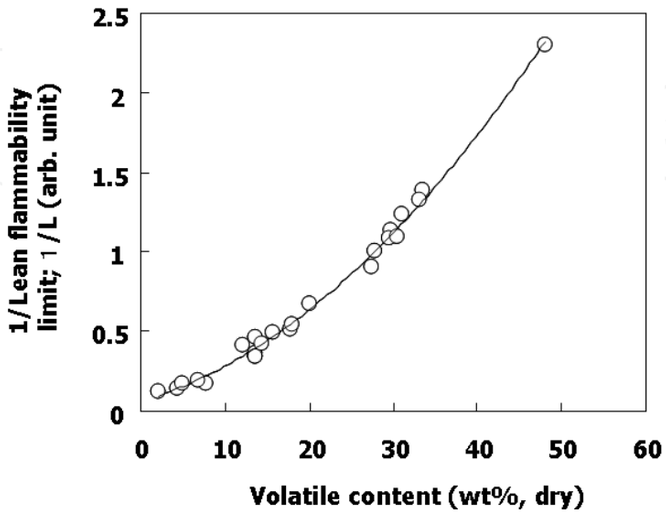

Fig. 9. Effects of coal properties on lean flammability limit.

The lean flammability limit of solid fuels is related to the pyrolysis rates and the amount of pyrolized fuel [24]. The lean flammability limit can also be evaluated by using pyrolysis experiments. Examples of pyrolysis calculations for various fuels are shown in Fig.10. The calculation method has been shown elsewhere [24, 25]. The relationship between heating time and amount of pyrolized volatile matter was calculated when the particle was heated at a rate of 20000K/s. The distributed activation energy model (DAEM) was used for the pyrolysis [24-29]. The pyrolysis rate dV/dt was calculated by Eq. (4).

$$\frac{dV}{dt} = V^{\infty} \int_0^{\infty} Av\, e^{-Ev/RTp}\, exp\,[-\int_0^t Av\, e^{-Ev/RTp(t')} dt\,]\; f(Ev)\, dEv \tag{4}$$

The initial mass of volatile matter V^{∞} was evaluated by Flashchain [29]. The function $f(Ev)$ shows the distribution of the activation energies and the frequency factor (Av). As shown in equations (5) and (6), $f(Ev)$ is expressed as a summation with more than one normal distribution function. The function $f(Ev)$ gives results that approximately agree with the experimental results for each coal type.

$$f(Ev) = \sum_{i=1}^{n} \frac{a_i}{\sqrt{2\pi}\, E\, \sigma_i}\; exp\,[-(E-Eav_i/2E\,\sigma_i^2] \tag{5}$$

$$\sum_{i=1}^{n} a_i = 1 \tag{6}$$

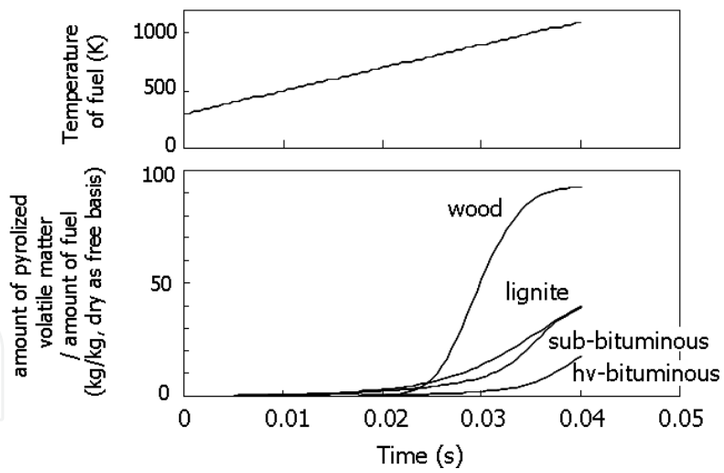

Fig. 10. Examples of pyrolysis calculation results for evaluating lean flammability limit.

In general, pyrolysis started at low temperature and the amount of pyrolized volatile matter increased when volatile content of fuel increased, as shown in Fig. 10. We assumed that L was in inverse proportion to the amount of pyrolized volatile matter

Figure 11 compares estimated L values based on the pyrolysis calculation with measured values. The pyrolysis rate constant was fitted by thermogravimetric analyses [27]. The estimated values agreed with the experimental values. Pyrolysis rates and amount of the pyrolized fuels was strongly related to lean flammability limits.

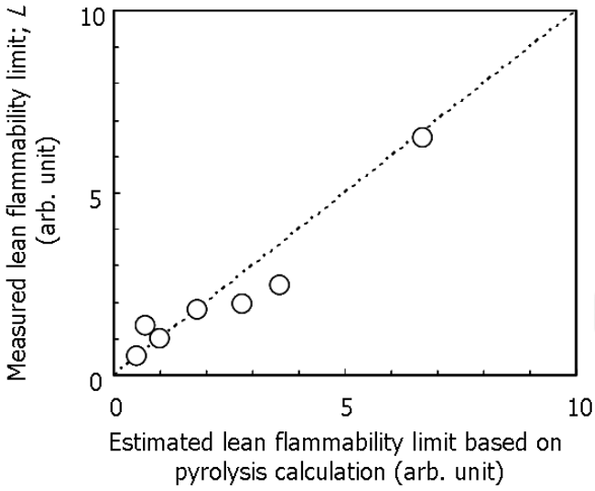

Fig. 11. Relationship between pyrolysis property and lean flammability limit. Estimated flammability limit based pyrolysis calculations are compared with measured lean flammability limits.

The particle diameter also strongly influences lean flammability limit. When the diameter is uniform, the lean flammability limit is proportional to the 1.5th power of the particle diameter and the maximum distance between particles for flame propagation is proportional to the square root of the diameter [11].
The solid fuels are ignited by the following.

1. The particles are heated from the surroundings
2. The particle temperature increases, then, volatile matter is pyrolized.
3. The concentration of pyrolized volatile matter increases, then, pyrolized volatile matter and particles ignite.

When the particle diameter is large, a rise of particle temperature in (2) becomes slow.

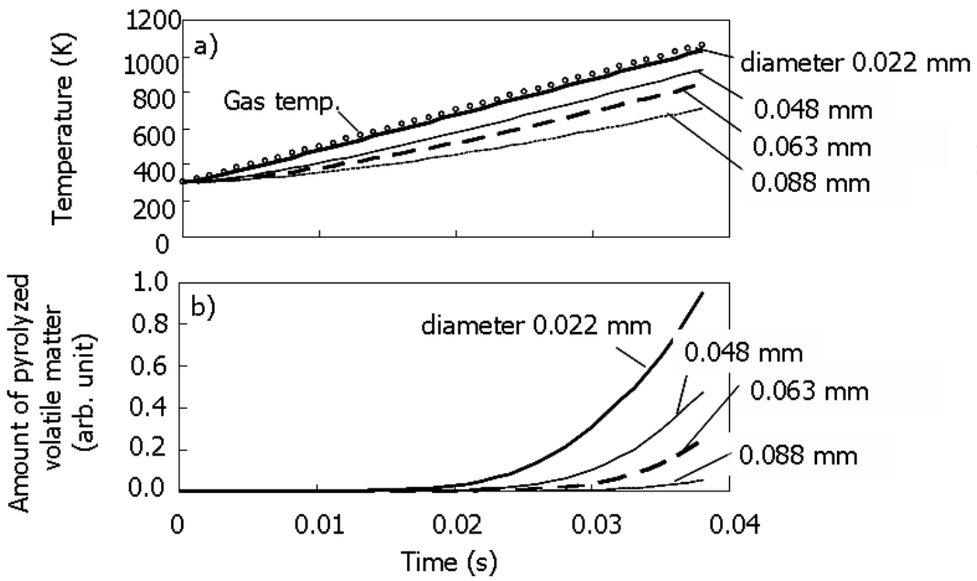

Fig. 12. Effect of particle diameter on pyrolysis property.

Effect of particle diameter on pyrolysis characteristics was examined. The results are shown in Fig.12. Pyrolysis processes were calculated when the surrounding gas temperature was heated at a constant rate. Heating rate of surrounding gas was 20000K/s. Figure 12(a) shows time changes of the amount of pyrolyzed volatile matter, and Fig. 12(b) shows time changes of the particle temperature.

The method of calculation has been shown elsewhere [27]. Heat balance of particles was written as

$$C_p \rho V_p \frac{dT_p}{dt} = Sh(T_g - T_p) - S\ \varepsilon\ \sigma(\ T_p^4 - T_w^4) \tag{7}$$

where Cp is specific heat of particles, h is convective heat transfer coefficient, Tg is gas temperature, T_p is particle temperature, T_w is wall temperature, S is external surface area of particles, ρ is particle density, ε is particle emissivity, and σ is the Stefan-Boltzmann constant. C_p was assumed to be the same as graphite, and taken from Merrick [30]. h was obtained by assuming that the Nusselt number was 2 [10]. T_w was 300K. ρ was assumed as 1.4 kg/m^3. $\varepsilon$was assumed as 0.8. σ was 5.67x10^{-8} W/m^{2}K^4.

Figure 12(a) shows time changes of the particle temperature. When particle diameter was small, 0.022 mm, particle temperature increased as soon as gas temperature rose. The gap between the particle temperature and the gas temperature was small. When the particle diameter became large, the rise in temperature became slow. Fig. 12(b) shows time changes of the amount of pyrolyzed volatile matter. Pyrolysis became slow when the particle diameter became large, so that ignition became difficult; i.e. lean flammability limit became large.

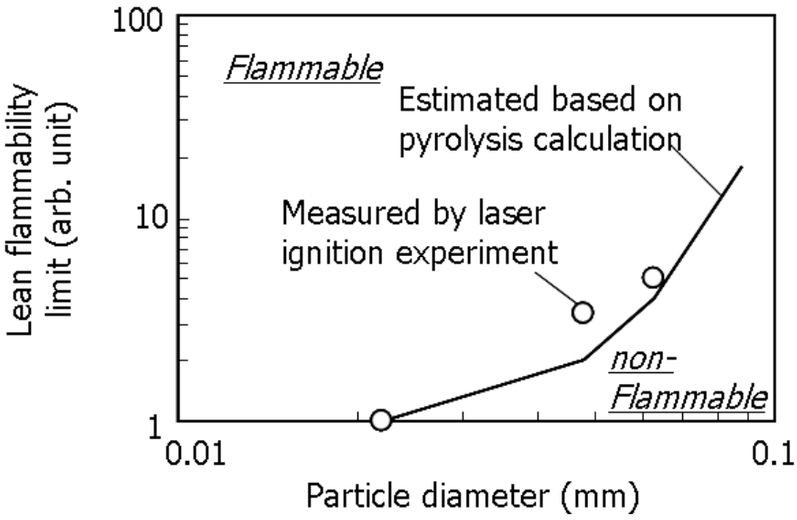

Fig. 13. Effect of particle diameter on lean flammability limit.

Figure 13 shows the relationship between particle diameters and estimated and measured lean flammability limits. Measured lean flammability limit increased with diameter. It was almost proportional to the 1.5th power of the diameter. Estimated results reproduced the tendency.

Recently, development of oxy-fuel combustion technology has been particularly active using pilot-scale plants [14]. Fundamental studies of ignition for oxy-fuel combustion have also been promoted [9, 31, 32]. Suda et al. [9] examined flame propagation velocity under N_2/O_2 and CO_2/O_2 surroundings. When the oxygen concentrations were the same, flame

propagation velocities for CO_2/O_2 combustion were lower than those for N_2/O_2 combustion; ignition became difficult for oxy-fuel combustion. Effect of surrounding gas composition should be modeled to allow application of ignition studies to oxy-fuel combustion systems.

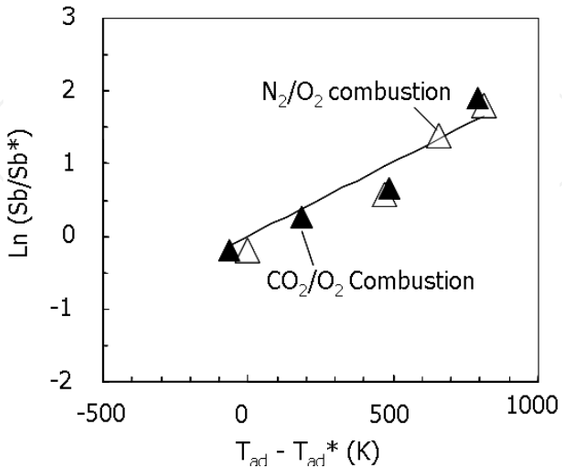

Fig. 14. Relationship between flame propagation velocity and flame temperature formed around the particle [12]. Experimental data were obtained from Suda et al. [9].

The experimental data have been analyzed by paying attention to the flame temperature formed around the particles [12]. Figure 14 shows the relationship between flame temperatures and maximum flame propagation velocities. T_{ad} in the horizontal axis is the adiabatic flame temperatures of volatile matter under the stoichiometry condition [12]. The maximum flame propagation velocity could be predicted from the flame temperature with no dependence on the surrounding gas composition. The relationship between maximum flame propagation velocity and lean flammability limit was already shown in Fig. 8, so that the lean flammability limit could also be predicted from the flame temperature.

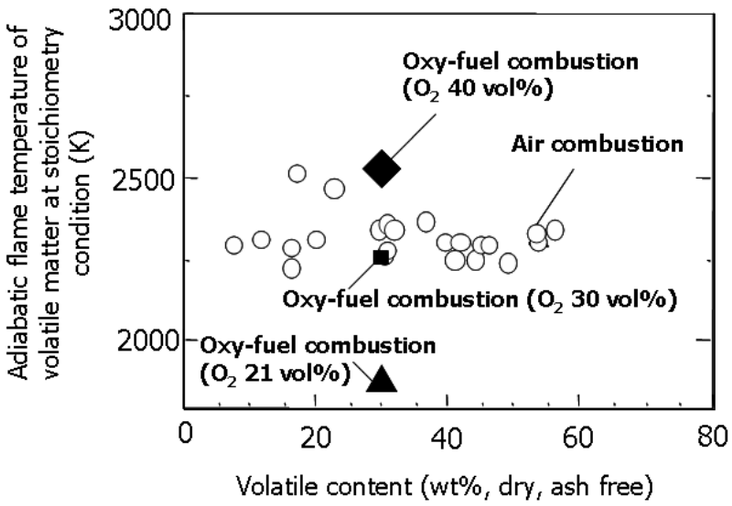

Fig. 15. Calculated adiabatic flame temperatures of volatile matter at stoichiometry condition, under various coals and surrounding gas compositions.

The primary reason why the flame propagation velocity for the CO_2/O_2 combustion was small is that the flame temperature was low, because the specific heat was large. Figure 15 shows adiabatic flame temperature of volatile matter for various coals. When the surrounding gas compositions were the same, effects of coal properties on the adiabatic flame temperatures were small. The adiabatic flame temperature varied when surrounding gas compositions was changed. When oxygen concentrations were the same, the adiabatic flame temperature for oxy-fuel combustion was lower than that of air combustion; ignition for oxy-fuel combustion was difficult. For oxy-fuel combustion, oxygen concentration should be increased to around 30%, in order to secure the same ignition performance as air combustion.

Based on these fundamental results, we developed the model to predict both flame propagation velocity and lean flammability limit [11, 24]. Verification examples are shown in Fig. 16. Calculated results agreed well for various coal properties and experimental conditions.

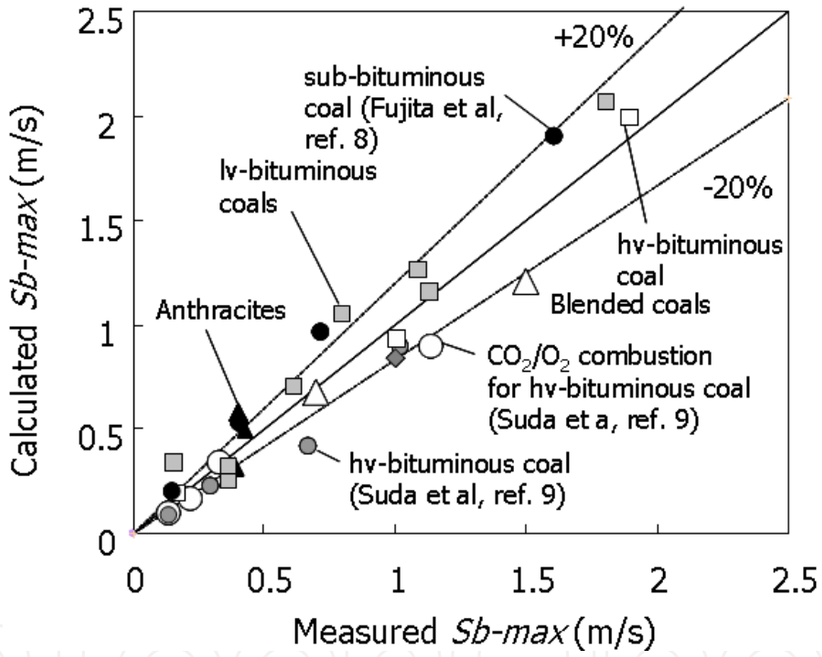

Fig. 16. Verifications of the developed flame propagation model.

3. Lift-off height measurement of pulverized coal jet flame ignited by a preheated gas flow

3.1 Experimental equipment

Lift-off height is usually used for an index of flame stability of continuous gas and liquid flames [33]. This index is used for verification of numerical calculations. However, it has not been examined for coal combustion using simulations. We developed an experimental apparatus to evaluate lift–off height of continuous coal flames, and LES (large eddy simulation) results were verified with the experimental results [23].

Figure 17 shows schematic drawings of the pulverized coal jet flame experiment [27]. The mixture of coal and air was injected through a primary nozzle installed at the centreline of

the preheated gas flow and ignited by the surrounding preheated gas. Maximum coal feed rate was 2 kg/h and maximum flow rate of primary air was 3 m^3N/h. The nozzle was made of stainless steel and consisted of two concentric tubes with an inner diameter of 7 mm and outer diameter of 25 mm. The injected coals were ignited in the combustion area (open area). Lift-off heights were observed by using a high-speed camera. The surrounding preheated gas was supplied though a honeycomb (100mm square, 30 mm thick) which was symmetrically placed around the nozzle exit. The surrounding gas was formed by catalytic combustion of propane [34]. At first, air was preheated to around 700K by the electrical heater. The preheated air and primary propane mixture was burned in the honeycomb catalyst. The burned gas was mixed with secondary propane downstream form the catalyst. Finally, the gas was heated to 1400-1600K by combustion of secondary propane on the SiC honeycomb. Maximum flow rate of the surrounding preheated gas was 36 m^3N/h.

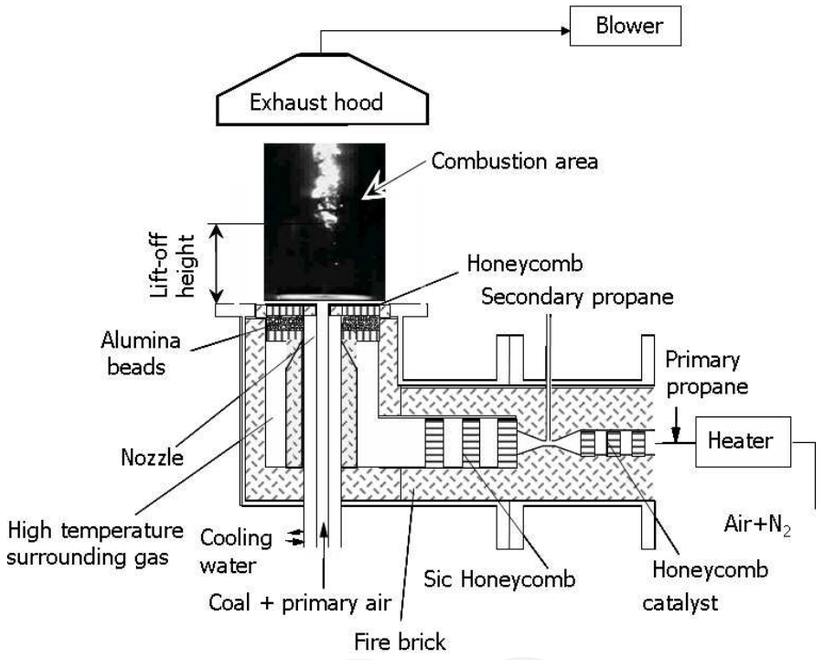

Fig. 17. Schematic drawing of an ignition experiment for lift-off height measurement of continuous flame.

The combustion gas flowed to the outlet through the exhaust hood and the duct. The Reynolds number of the primary jet was about 4500. The inlet stoichiometric ratio (*SR*) is the most important operating parameter for ignition in this experiment. Downstream from the outlet, a blower vigorously sucked in flue gas. Thus some air was taken from the open area. Prior to the experiment, the amount of the suction flow was estimated from the difference between the amount of the flue gas at the blower and the amounts of the primary air and the preheated gas. The velocity on the side boundary was estimated as 0.16 m/s.

3.2 Flame structure

Figure 18 shows a series of photos showing the ignition process of hv-bituminous coal. Figure 18(a) reproduces instantaneous photos and (b) is the averaged photo. Coal particles were ignited around 150mm downstream from the burner exit [27, 35]. Burning coal

particles were not observed from the burner exit to 150mm downstream. Coal particles were preheated by surrounding gas in this region. Small flames were observed at 150 mm. These small flames grew further downstream, and, formed large flames. A large continuous flame was observed at 200-300 mm. These flame growth phenomena were similar to flame propagation phenomena observed by the laser ignition experiments. The averaged photo showed that the flame luminousness started to increase around 150mm. Lift-off height was defined as the distance between the burner exit and the position that the flame luminousness started to increase.

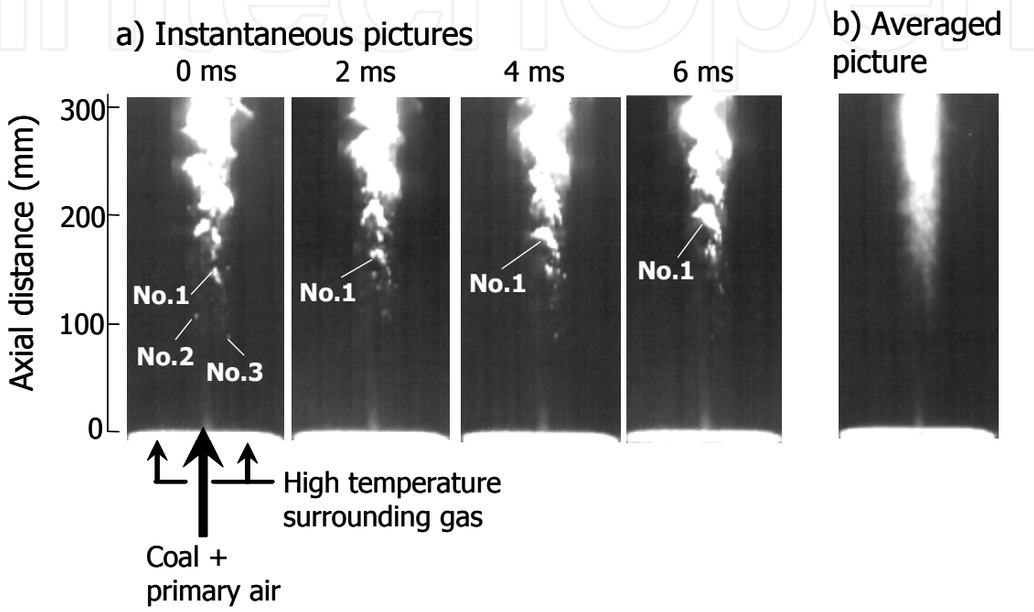

Fig. 18. Example series of flame photos of pulverized coal ignition. Coal particles were ignited by injecting high temperature gas flow.

Figure 19 shows gas temperature, gas composition, and coal burnout profiles along the center axis. Coal concentration in the primary air for Fig. 19 was lower than that for Fig. 18, so that, lift-off height of Fig. 19 was larger than that of Fig.18. Figure 19(a) shows coal burnout profiles. Volatile content of the coal was around 35vol% (dry, ash-free basis). Pyrolysis of fine coals (<0.037 mm) began before ignition. Particle diameter was a very important factor for ignition. The combustible gas formed by pyrolysis of fine particles was strongly related to ignition [23, 27]. Pyrolysis of intermediate size coals (0.037-0.074 mm) began at the ignition region where the small flames formed and grew. Pyrolysis of large coals (>0.074 mm) began after a large continuous flame was formed. The fine particles could strongly contribute to promotion of ignition. The intermediate size particles could also contribute, but, the effect was not large. The large particles could not contribute very much.
Figure 19(b) shows gas temperature profiles. A profile when coal was not supplied is shown for comparison. When the luminous flame was formed, the heat of coal combustion was released, so that the gas temperature when coal was present was larger than that without coal. Figure 19(c) shows O_2 and NOx concentration profiles. Oxygen consumption began when the luminous flame was formed. NOx concentration started to increase rapidly after ignition. The rise of NOx is a good index to judge ignition [3].

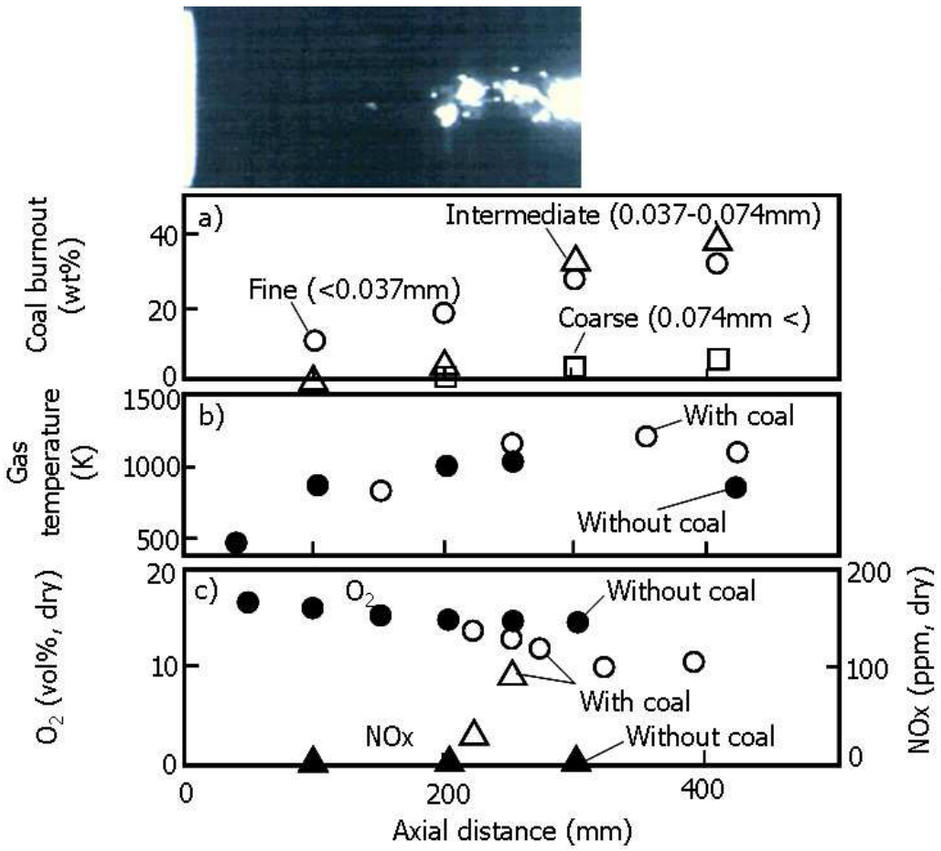

Fig. 19. Axial profiles of coal burnout, gas temperature, O_2 and NOx in the ignition area of coal combustion.

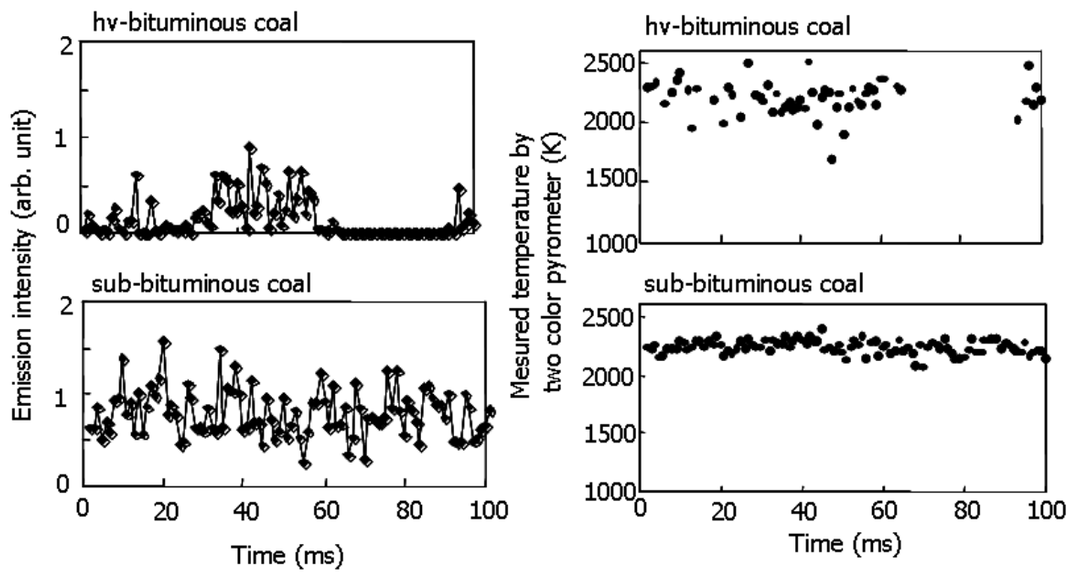

Fig. 20. Particle emission intensity and temperature in the ignition area of hv-bituminous and sub-bituminous coal flames. Particle temperature was measured using a two-color pyrometer.

Particle temperatures (or soot temperature of coal flames formed around the particle) in the ignition region were measured by a two-color pyrometer. The results are shown in Fig.20. Emission intensities and particle temperatures of hv-bituminous and sub-bituminous coals were measured. Emission intensity of sub-bituminous coal was larger than that of hv-bituminous coal. Measured particle temperatures of the two kinds of coals were almost the same. Measured temperatures were around 2200-2300K. These values were almost the same as the adiabatic temperature of the volatile flame formed around the particle (Fig. 15). Averaged gas temperature in the ignition region was around 1000-1300K (Fig. 19). When the coal ignited, particle temperature increased rapidly.

3.3 Relation between the experiments of continuous flames and the laser ignition experiments

In Section 2, we described verification of the flame propagation velocity and lean flammability limit model by laser ignition experiments; these were for unsteady combustion. Then here we verified whether this model could be applied for examination of flame stability for stable flames. Lift-off height is usually used for an index of flame stability. Yamamoto et al. [23] have examined the effect of coal concentration on lift-off height for coal combustion by LES. The flame propagation velocity and lean flammability limit model could successfully evaluate the relationship between coal concentration and flame propagation velocity. They showed that if flame propagation velocity was large, coal could ignite easily.

Lift-off heights were measured for three different primary coal concentrations. Results are shown in Fig.21. The horizontal axis is the calculated flame propagation velocity at the burner exit. A good relationship was observed between calculated flame propagation velocity and lift-off height. When coal concentration increased, flame propagation velocity rose, so that lift-off height became short because coal ignition became easy. Fig. 21 shows results for hv-bituminous coal. A similar conclusion has been obtained for lv-bituminous coal [24]. The flame propagation velocity and lean flammability limit model could also be applied for continuous and stable flames.

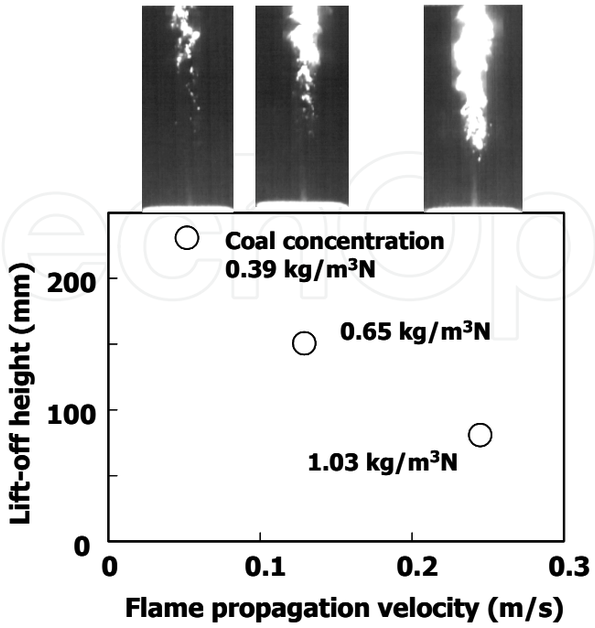

Fig. 21. Effect of primary coal concentration on lift-off height of hv-bituminous coal flames.

4. Application to burner development

In Section 2, we developed the flame propagation velocity and lean flammability limit model by analyzing the result of the laser ignition experiments. In Section 3, the model was applied to examine flame stability of the stable continuous flames. In this section, we paid attention to engineering designs of commercial or pilot scale systems.

Figure 22 is a schematic of the actual boiler and burner arrangement [21]. Blow-off limit fuel concentration of the installed burner is an important design parameter. However, it is not easy to measure the blow-off limits for large scale burners. Development of the model is required to predict the blow-off limits for various burning conditions from limited experimental data.

For actual systems, plural burners are usually installed in one furnace. An example of the burner arrangement is shown on the right side of Fig.22. Heat loss rate from the ignition region of the flames to the furnace wall for actual systems is different from that for small scale equipment. Usually, the heat loss rate for actual systems is small, because one flame is heated by other flames in the neighborhood. Furnace water wall temperature is usually high for actual systems. The influence of radiant heat loss on flame stability should be modeled.

At first, we simulated the influence of radiant heat flux from surroundings to the flame by using the laser ignition equipment. Figure 23 shows the relationship between the radiant heat flux and lean flammability limit. The radiant heat was given by irradiating a continuous laser to the floating pulverized coal particles (Fig.3). The radiant heat flux was regulated by controlling the power of the continuous laser. Usually, the water wall temperature of boilers is 600-700K, and this is equivalent to 1-2 x10^4 W/m2 of heat flux. The heat flux rose more when one flame received radiant heat from other flames.

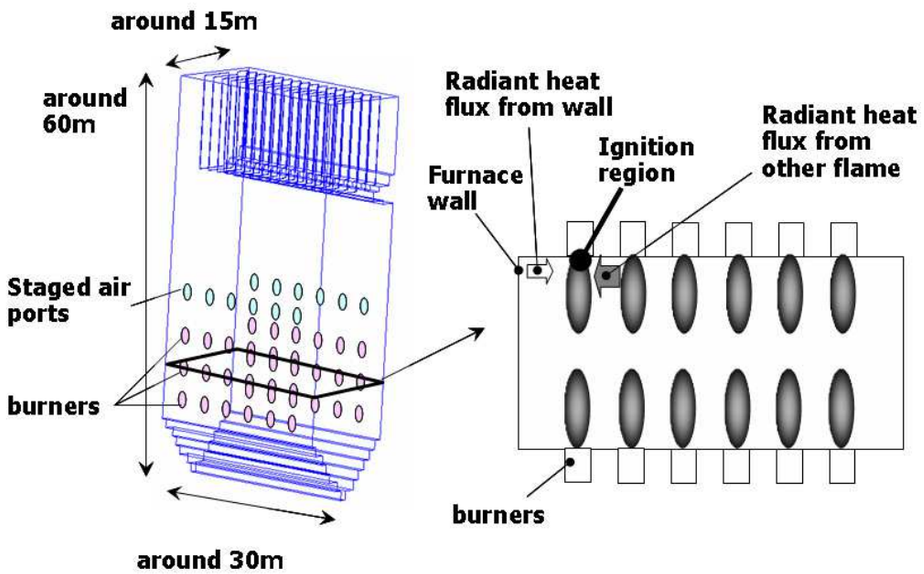

Fig. 22. Example burner arrangement of a pulverized coal fired boiler.

According to Fig. 23, the basic expression of the influence of the radiant heat flux was Eq. (8)[21]

$$1/L = 1/L_0 + a\,Ra \tag{8}$$

where L is lean flammability limit, L_0 is lean flammability limit for the standard condition, Ra is radiant heat flux, and a is a constant.

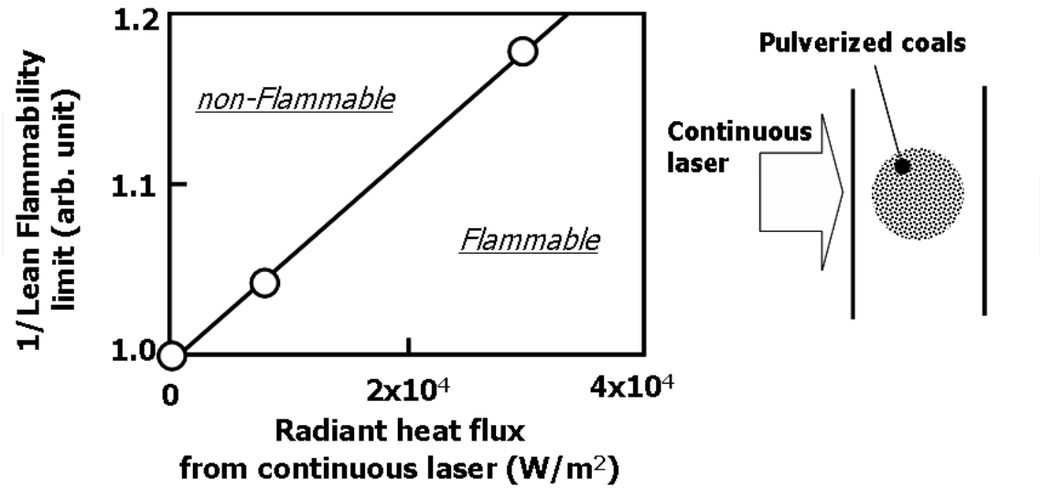

Fig. 23. Effect of radiant heat flux from surroundings to flame on lean flammability limit [21].

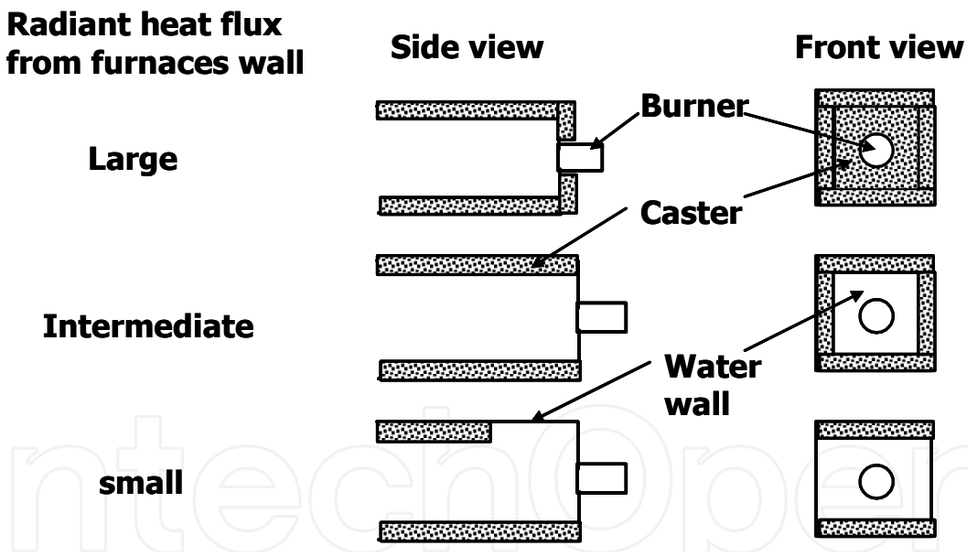

Fig. 24. Example of procedure to evaluate the effect of the radiant heat flux for large scale burners [36].

Figure 24 is an example of the procedure to measure influence of the heat loss by using pilot-scale burners [36]. The pilot-scale burners were almost the same size as for commercial-scale boilers; however, the number of installed burners was smaller. In many case, one large burner was installed for the pilot-scale furnaces. When one burner was installed in the furnace and was surrounded by a water wall, the radiant heat flux from the surroundings was lower than that for commercial-scale boilers. In order to simulate the radiant heat flux for commercial-scale boilers, a part of the furnace wall was surrounded by a caster wall. The effect of the radiant heat flux on flame stability could be evaluated by

varying the area of the caster wall. Blow-off limit for commercial-scale boilers could be analyzed from the experimental data by using Eq. (8) [21].
Figure 25 shows the relationship between fuel properties and blow-off limit fuel concentration. The developed model shown in Sections 2 and 3 could predict the effects of fuel properties, particle diameters, and surrounding gas conditions. Blow-off limit (lean flammability limit for actual boiler conditions) could be evaluated by adding the influence of the radiant heat flux. The results of Fig.25 showed that calculated results agreed with experimental results for anthracite, lv-bituminous coals, and hv-bituminous coals [25].
If calculations are verified for several kinds of fuels, blow-off limits for other fuels can be evaluated. Calculated results of blow-off limit for some wood powders are also shown in Fig.25. Biomass fuels are started to be used as an alternative fuel for pulverized coal fired boilers [37]. One of the problems with their use however was that fine grinding was difficult. If the blow-off limit for biomass fuels can be predicted, an appropriate grinding condition can be decided beforehand.

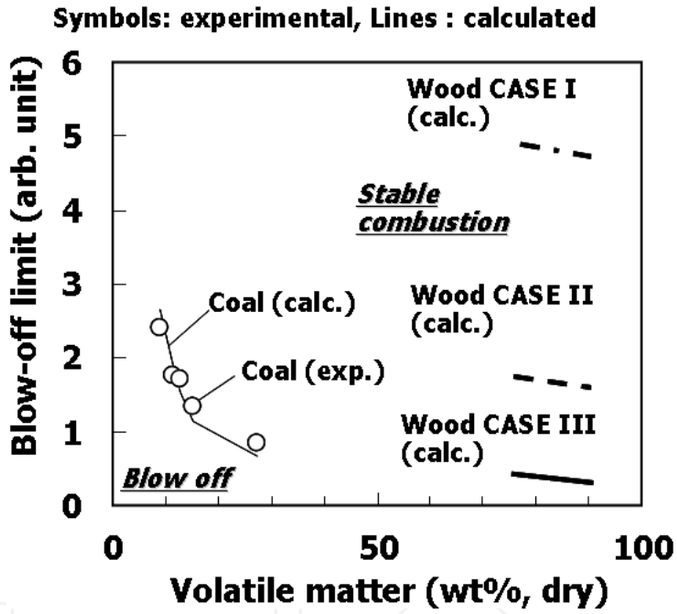

Fig. 25. Effects of coal properties on lean-blow-off limit for a large scale burner.

The effects of diameter on ignition performances for the wood powder were examined in detail. Figure 26(b) shows relationships between fuel concentrations and flame propagation velocities. Figure 26(a) shows diameter distributions for wood powders and hv-bituminous coal used for the case studies. The results for four wood powders and one hv-bituminous coal are shown. Hv-bituminous coal is used widely as fuel for boilers. If flame propagation velocity of the biomass fuel is the same as that of hv-bituminous coal, this biomass fuel is easy to use. Among CASEs I - IV, flame propagation velocity of CASE IV was almost the same as for that of hv-bituminous coal and the diameter distribution of CASE IV was appropriate.
Lift-off height of CASE IV was compared with that of hv-bituminous coal experimentally. The results are shown in Fig. 27. Fuel concentrations were the same. Lift-off height of CASE IV was almost the same level as that of bituminous coal, so that CASE IV was appropriate as the alternative fuel for pulverized coals.

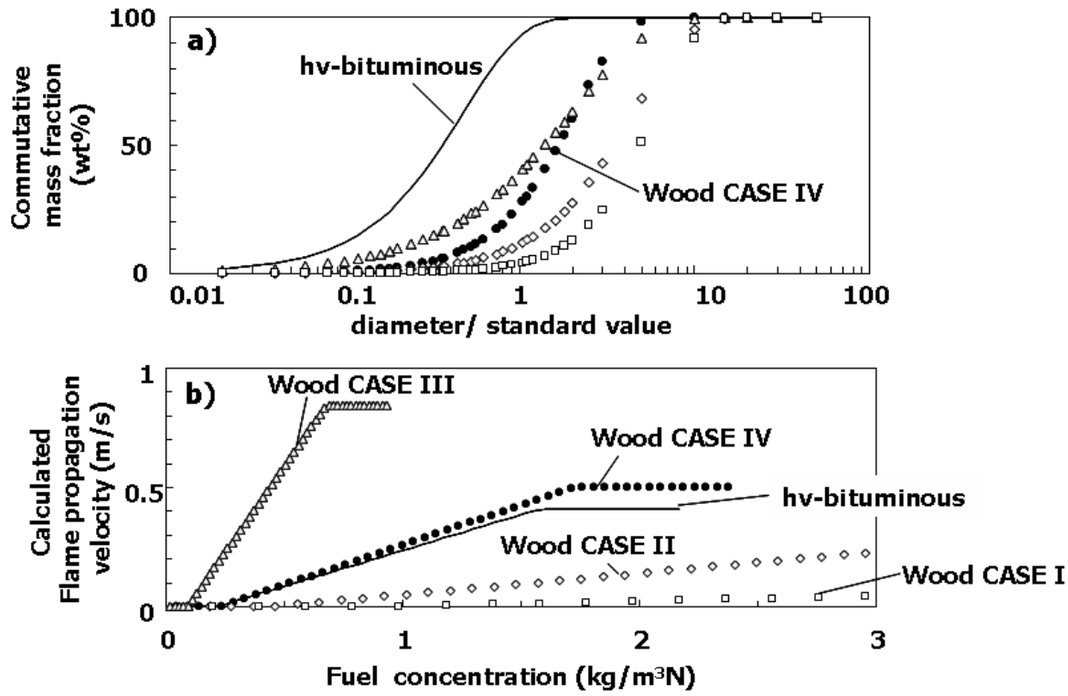

Fig. 26. Relationships between fuel concentration and calculated flame propagation velocities for various coal and wood powders.

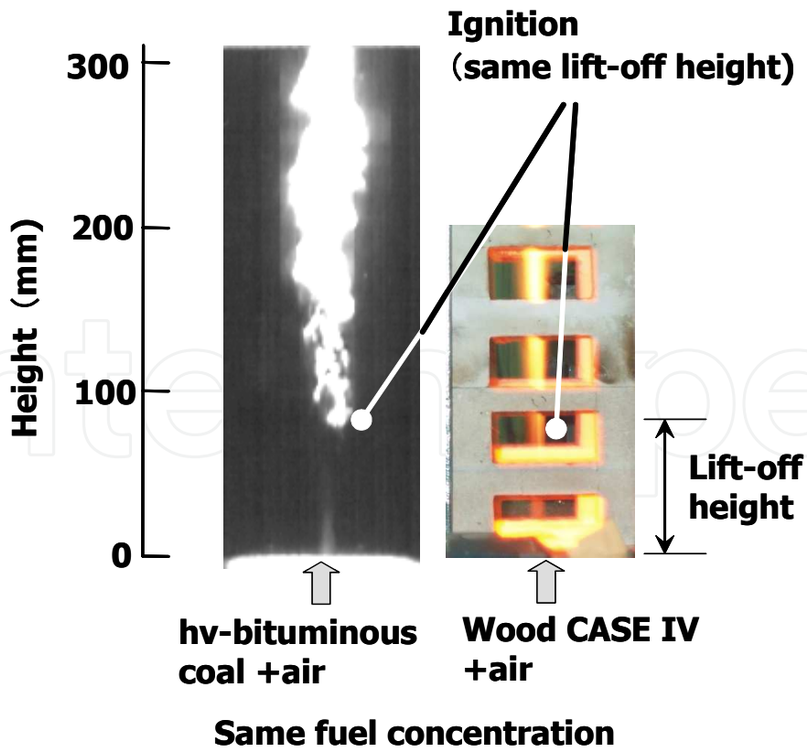

Fig. 27. Comparison of lift-off heights between hv-bituminous coal and wood powder for the same primary fuel concentrations.

5. Conclusion

Application of fundamental ignition experiments for a flame stabilization study was examined for engineering design of coal power plants. A model to evaluate flame stability of small scale experiments and large scale burners was developed based on the fundamental experimental results.

1. A flame propagation velocity and lean flammability limit model for pulverized solid fuels was developed by analyzing fundamental experimental results obtained in laser ignition experiments. The model could predict the effects of fuel properties, particle diameters and surrounding gas compositions on flame propagation velocity and lean flammability limit.
2. The model could be applied for flame stabilization study of coetaneous stable flames. Lift-off height of continuous coal flames could be evaluated from calculated flame propagation velocity by using the model.
3. The model could evaluate blow-off limit of large scale burners. It was found important to evaluate the difference between the effect of heat loss rate of small scale equipment and large scale burners. Case studies were introduced to obtain stable combustion for some biomass fuels.

6. Nomenclature

Av: frequency factor of pyrolysis	(1/s)
C_p: specific heat of particles	(J/kg K)
D_p : coal particle diameter	(m)
Eav_i: average activation energy	(kJ/mol)
Ev: activation energy of the pyrolysis	(kJ/mol)
$E\sigma_i$: standard deviation of activation energy	(kJ/mol)
h: convective heat transfer coefficient	(W/m^2 K))
L: lean flammability limit	(kg/m^{3}N)
R: gas constant = 8.314	(J/mol K)
Ra: radiant heat flux from surroundings to flame	(W/m^2)
S: external surface area of particles	(m^2)
Sb: flame propagation velocity	(m/s)
Sb-max: maximum flame propagation velocity	(m/s)
SR: stoichiometric ratio	(-)
T_g: gas temperature	(K)
T_p: particle temperature	(K)
T_w: wall temperature	(K)
V : amount of volatile matter at an instant in the pyrolysis	(kg)
V_p: volume of particle	(m^3)
V^∞: initial amount of volatile matter	(kg)
a_i: constant	(-)
b: constant	(-)
d: distance between coal particles	(m)
n: number of distribution functions of activation energy	(-)
s: flame propagation time	(s)
t: time	(s)

ε: emissivity of particle (-)
ρ: particle density (kg/m^3)
σ: Stefan-Boltzmann constant; 5.67×10^{-8} W/m^2K^4
Subscripts
i: i th component of volatile matter

7. References

[1] Chen, Y.; et al (1996). *Studying the mechanisms of ignition of coal particles by TG-DTA*, Thermochimica Acta, 275, 149-158.

[2] Tognotti, L; et al (1985). *Measurement of ignition temperature of coal particles using a thermogravimetric technique*, Combust. Sci. Tech., 44, 15-28.

[3] Wall, T. F; et al (1988). *Indicatiors of Ignition for Clouds of Pulverized Coal,* Combust. Flame, 72, 111-118.

[4] Cashdollar, K.L; (1996). *Coal dust explosibility,* Journal of Loss Prevention in the Process Industries, 9, 65-76.

[5] Cashdollar K.L. &. Hertzberg, M; (1983). *Infrared temperature of coal dust explosions,* Combust. Flame, 51, 23-35.

[6] G. E. Andrews and D. Bradley, The burning velocity of methane-air mixtures, Combust. Flame, 19 (1972) 275-288.

[7] Peeters, N; (1999). *The turbulent burning velocity for large-scale and small-scale turbulence*, Journal of Fluid Mechanics, 384, 107-132.

[8] Fujita, O; et al (1993). *HTD-vol. 269, Heat Transfer in Microgravity,* ASME 1993, 59-66.

[9] Suda, T; et al (2007). *Effect of carbon dioxide on flame propagation of pulverized coal clouds in CO_2/O_2 combustion*, Fuel, 86, 2008-2015.

[10] Chen, J. C; et al (1994). *Laser ignition of pulverized coals,* Combust. Flame, 97, 107-117.

[11] Taniguchi, M; et al (1996). *Laser ignition and flame propagation of pulverized coal dust clouds,* Proc. Combust. Inst., 26, 3189-3195.

[12] Taniguchi, M; et al (2011). *Prediction of lean flammability limit and flame propagation velocity for oxy-fuel fired pulverized coal combustion*, Proc. Combust. Inst. 33, 3391-3398.

[13] Ikeguchi, T; et al (2010). *Development of Electricity and Energy Technologies for Low-Carbon Society*, Hitachi Review, 59, 53-61.

[14] Wall, T; et al (2011). *Demonstrations of coal-fired oxy-fuel technology for carbon capture and storage and issues with commercial deployment,* International Journal of Greenhouse Gas Control, (2011) Volume 5, Supplement 1, July 2011, Pages S5-S15, doi:10.1016/j.ijggc.2011.03.014

[15] Ochi, K; et al (2009). *Latest Low-NOx Combustion Technology for Pulverized-coal-fired Boilers,* Hitachi, Review, 58, 187-193.

[16] Iwashige, K; et al (2008). *Numerical simulation for electric power plant systems,* Hitachi Hyoron, 90, 66-71.

[17] Ito, O; et al (2008). *CO_2 reduction technology for thermal power plant system*, Hitachi Hyoron, 90, 20-25.

[18] Handa, M; et al (2008). *Numerical method for three-dimensional analysis of shell-and –tube type of large scale heat exchangers under high temperature circumstances*, Advances in computational heat transfer, CHT-08.

[19] Yamamoto, K; et al (2000). *Development of Computer Program for Combustion Analysis in Pulverized Coal Fired Boilers*, Hitachi Review 49, 76-80.

[20] Yamamoto, K; et al (2005). *Validation of coal combustion model by using experimental data of utility boilers*, JSME International Journal Series B, 48, 571-578.

[21] Taniguchi, M; & Yamamoto, K; (2010). *Fundamental research on oxy-fuel combustion: The NOx and coal ignition reactions.* In: Grace CT, (Ed.), Coal Combustion Research, Nova Science Publishers Inc., New York, pp59-69.

[22] Phillips, S; et al. *Application of high steam temperature countermeasures in high sulfur coal-fired boilers,* available at the address: http://www.hitachi.powersystems.us/supportingdocs/forbus/hpsa/technical_papers/EP2003B.pdf.

[23] Yamamoto, K; et al (2011). *Large eddy simulation of a pulverized coal jet flame ignited by a preheated gas flow*, Proc. Combust. Inst. 33, 1771-1778.

[24] Taniguchi, M; et al (2011). *Application of lean flammability limit study and large eddy simulation to burner development for an oxy-fuel combustion system*, International Journal of Greenhouse Gas Control, Volume 5, Supplement 1, July 2011, Pages S111-S119. doi:10.1016/j.ijggc.2011.05.008

[25] Taniguchi, M; et al (2009). *Comparison of flame propagation properties of petroleum coke and coals of different rank*. Fuel, 88, 1478-1484.

[26] Chen, J. C; et al (1995). *Observation of laser ignition and combustion of pulverized coals*, Fuel, 74, 323-330.

[27] Taniguchi, M. et al (2001). *Pyrolysis and ignition characteristics of pulverized Coal Particles.* ASME Journal of Energy Resources Technology, 123, 32-38.

[28] Niksa S; & C.-W. Lau, C.-W; (1993). *Global rates of devolatilization for various coal types.*, Combust. Flame, 94, 293–307.

[29] Niksa, S; (1995). *Predicting the devolatilization behavior of any coal from its ultimate analysis*, Combust. Flame, 100, 384-394.

[30] Merric, D; (1983). *Mathematical models of the thermal decomposition of coal: 2. Specific heats and heats of reaction*, Fuel, 62, 540-546.

[31] Arias, B; et al (2008). *Effect of Biomass Blending on Coal Ignition and Burnout during oxy-fuel Combustion*., Fuel, 87, 2753-2759.

[32] Shaddix, C. R; & Molina, A; (2009). *Particle imaging of ignition and devolatilization of pulverized coal during oxy-fuel combustion,* Proc. Combust. Inst., 2091-2098.

[33] Peters, N; (2000). *Turbulent Combustion,* Cambridge University Press, Cambridge, pp. 238-245.

[34] Maruko, S; et al (1994). *Multistage Catalytic Combustion Systems and High temperature Combustion Systems using SiC*, Catalysis Today, 26, 107-117

[35] Taniguchi, M; et al (2000). *Ignition process of pulverized coal Injected into preheated gas flow*, Kagaku Kogaku Ronbunshu, 26, 194-201.

[36] Kiga, T; et al (1987). *Development of IHI Wide Range Pulverized Coal Burner,* Ishikawasjima Harima Giho, 27, 333-338.

[37] Wang, X; et al (2011). *Experimental investigation on biomass co-firing in a 300 MW pulverized coal-fired utility furnace in China*, Proc. Combust. Inst., 33, 2725-2733.

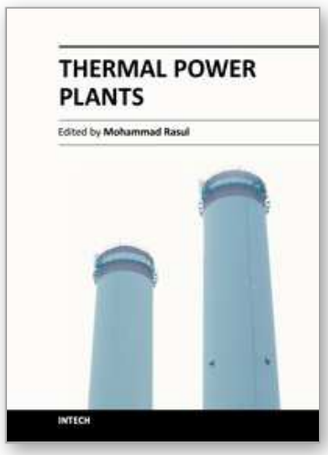

Thermal Power Plants

Edited by Dr. Mohammad Rasul

ISBN 978-953-307-952-3
Hard cover, 266 pages
Publisher InTech
Published online 13, January, 2012
Published in print edition January, 2012

Thermal power plants are one of the most important process industries for engineering professionals. Over the past few decades, the power sector has been facing a number of critical issues. However, the most fundamental challenge is meeting the growing power demand in sustainable and efficient ways. Practicing power plant engineers not only look after operation and maintenance of the plant, but also look after a range of activities, including research and development, starting from power generation, to environmental assessment of power plants. The book Thermal Power Plants covers features, operational issues, advantages, and limitations of power plants, as well as benefits of renewable power generation. It also introduces thermal performance analysis, fuel combustion issues, performance monitoring and modelling, plants health monitoring, including component fault diagnosis and prognosis, functional analysis, economics of plant operation and maintenance, and environmental aspects. This book addresses several issues related to both coal fired and gas turbine power plants. The book is suitable for both undergraduate and research for higher degree students, and of course, for practicing power plant engineers.

INTECH
open science | open minds

InTech Europe
University Campus STeP Ri
Slavka Krautzeka 83/A
51000 Rijeka, Croatia
Phone: +385 (51) 770 447
Fax: +385 (51) 686 166
www.intechopen.com

InTech China
Unit 405, Office Block, Hotel Equatorial Shanghai
No.65, Yan An Road (West), Shanghai, 200040, China
中国上海市延安西路65号上海国际贵都大饭店办公楼405单元
Phone: +86-21-62489820
Fax: +86-21-62489821

IntechOpen